

UCRL-JC-115713

Preprint

# The Multifragmentation Freeze-Out Volume in Heavy Ion Collisions

G. Peilert, T.C. Sangster, M.N. Namboodiri, and H.C. Britt

Lawrence Livermore National Laboratory,  
Livermore, CA 94550  
USA

September 9, 2018

**Abstract:**

The reduced velocity correlation function for fragments from the reaction  $\text{Fe} + \text{Au}$  at 100 A MeV bombarding energy is investigated using the dynamical-statistical approach QMD+SMM and compared to experimental data to extract the Freeze-Out volume assuming simultaneous multifragmentation. It is shown that the data are consistent with a Freeze-Out volume corresponding to  $0.1 - 0.3$  times normal nuclear matter density. The calculations show an additional correlation due to recoil effects from a heavy third fragment in an asymmetric break-up. This effect is present, but less pronounced in the data.

A topic of great interest in nuclear physics is the multifragmentation of heavy nuclei at moderate excitation energies. Such systems are typically formed in p-nucleus reactions in the GeV energy regime or in intermediate energy heavy ion collisions. In the experiments of the Purdue group [1], first attempts were made to relate the inclusive results from p-nucleus fragmentation to the critical exponents of a phase transition, analogous to the liquid gas transition in condensed matter physics. Within the last few years it has become possible to study such reactions in highly exclusive experiments in order to extract the critical properties. Critical properties can then be extracted investigating by, for example the moments of the mass distribution as proposed by Campi [2].

Such a procedure, however can not provide the physical quantities that drive this phase transition. If one wants to extract quantities like a critical temperature and density one has to rely on dynamical models. Unfortunately there is presently no complete model available that describes the process of thermally driven multifragmentation in heavy ion collisions in a consistent approach. Current modeling involves a two-step dynamical-statistical process beginning with a pre equilibrium stage described in the earliest approaches by an Intranuclear Cascade Model [3] and, more recently, by molecular dynamics pictures such as the Quantum Molecular Dynamics model, QMD [4, 5] or by single particle models of the VUU/BUU type [6]. Following this stage there remains a distribution of nucleons and complex fragments which can themselves be highly excited and will undergo further statistical decay. This statistical decay process has been modeled in various codes as a sequential evaporation [7, 8, 9] or as an explosive simultaneous multifragmentation [10, 11, 12, 13, 14]. None of these models, however, includes the dynamics of the fragmentation.

Recent investigations with the QMD model have shown that for central collisions of heavy nuclei at high energies, a rapid compression-decompression mechanism emerges in the initial stage of the reaction and leads to a direct multifragmentation process, where a highly excited heavy residue is no longer formed with high probability [5, 15]. These investigations suggest that the region to search for the thermally driven multifragmentation in heavy ion reactions is in central collisions at moderate bombarding energies ( $E/A \approx 100$  A MeV) or in peripheral (or highly asymmetric) reactions at higher energies ( $E/A \approx 1$  A GeV). Under these conditions the direct reaction leads to a highly excited source that then breaks up into many IMF's.

Recently, attempts have been made by Sangster et al., [16] and Lacey et al. [17] to extract the emission time scale of the multifragmentation process by assuming a sequential decay mechanism with a fixed Freeze-Out volume. In contrast to earlier work performed by Kim et al. [18] using the Koonin-Pratt formalism [19] they used a the classical three-body trajectory code *MENEKA* [20] to simulate the sequential emission of IMF's from the surface of a spherical source characterized by a unique radius parameter. In this Letter we will show, that the same data can be explained by assuming a simultaneous multifragmentation from a Freeze-Out volume considerably larger than the ground state dimension.

This will be done by using the QMD+SMM approach. In this case the Hamilton equations of all nucleons are integrated, which implies that correlations between all the existing nucleons and fragments are treated in all orders. This is especially important in the case when one

deals not only with two IMF's, but with many. In the following we present comparisons of the QMD+SMM fragment-fragment correlation function for the reaction Fe (100 A MeV) + Au for central collisions ( $b = 0 - 6$  fm) in to the data of Ref. [21]. After the break-up of the hot target remnant within the SMM model (after 300 fm/c reaction time) we neglect the nuclear forces and follow the Coulomb trajectories of the charged particles through an experimental acceptance filter.

The QMD+SMM approach models the dynamical reaction and subsequent statistical decay of the excited pre fragments (details about the two models can be found in refs. [5, 21, 12]). Previous investigations with the QMD model [5] have shown that there are two different mechanisms leading to the multifragmentation. One is related to the mechanical rupture of the system whenever compressional effects are important; the other produces fragments thermally from an equilibrated source. This thermal multifragmentation has so far not been described in a microscopic model like QMD [5]. In the first comparison to inclusive IMF data it was shown that a two-step model was necessary to reproduce the experimental angular distributions [21]. This two-step model involved the calculation of initial kinematics and excitation energy of all pre fragments with the QMD model followed by a subsequent deexcitation calculation utilizing the Statistical Multifragmentation Model (SMM) of Botvina et al. [12]. The input for the SMM stage of the reaction, i.e., the mass and the excitation energy of the fragments, are consistently determined within the QMD approach.

The SMM model describes the multifragmentation of highly excited nuclei based on the statistical approach and a liquid-drop description of hot fragments. It is assumed that the excited primordial fragments break up into an assembly of nucleons and fragments. All these decay products are described as Boltzmann particles in a Freeze-Out volume  $V = V_0(1 + \kappa)$ , where  $\kappa$  is a model parameter and  $V_0$  is the volume of the system corresponding to normal nuclear matter density. Since all the produced fragments are excited (only particles with  $A \leq 4$  are considered as elementary particles) the final deexcitation is treated as a Fermi break up for lighter fragments ( $A < 16$ ) and via an evaporation of nucleons and clusters up to  $^{18}\text{O}$  for heavier fragments (for details see Ref. [12]). In the following we will vary the volume parameter  $\kappa$  from 1 to 15 in order to extract the Freeze-Out volume by comparing the reduced velocity correlation functions for each value of  $\kappa$  with the experimental data.

Figure 1 shows a comparison between the experimental data [21] and the QMD+SMM calculations using  $\kappa = 2, 5$  and 10 for two different projections of the double differential cross section,  $d^2\sigma/dZ/d\Omega$ . Both the data and the calculations are for central collisions only (for details see Ref. [21]). The upper part of figure 1 shows the charge yield distribution at a laboratory angle of  $72^\circ (\pm 13^\circ)$ , while the lower part shows the angular distribution of fragments with  $Z=10$ . In both cases it can be seen that the variation of the volume parameter  $\kappa$  does not influence these semi-exclusive observables and all calculations agree reasonably well with the data. However, the calculated angular distributions are still somewhat too steep and under predict the data at backward angles.

The reduced velocity correlation functions shown in figure 2 have been obtained by taking the ratio of the correlated reduced velocity distribution and a background distribution obtained by

event mixing between correlated IMF's in a single event divided by the same quantities obtained from two IMF's from different physical events, thereby eliminating final state correlations. In all cases the true ( $Y_{true}(v_{red})$ ) and background distributions ( $Y_{back}(v_{red})$ ) were developed separately for two classes of events: 1) two IMF's detected on opposite sides of the beam and, 2) two IMF's detected on the same side of the beam. In the areas where these two correlation functions overlap in relative velocity it was found that the correlations obtained were effectively identical and so in this paper the results have, in all cases, been combined into single distributions. The two fragment correlation function is then calculated according to

$$1 + R(v_{red}) = \frac{Y_{true}(v_{red})}{Y_{back}(v_{red})}. \quad (1)$$

Fig. 2 shows the experimental correlation function (symbols) for the three different charge product bins  $Z_1 \cdot Z_2 = 25 - 64$ ,  $65 - 129$  and  $130 - 250$  (the smallest detected charge is  $Z=5$  in all cases) compared to the calculated results (lines) for different volume parameters  $\kappa$  in the SMM model (recall that  $V = V_0(1 + \kappa)$ ). The curves show fits to the theoretical correlation functions using the fitting function

$$1 + R(v_{red}) = a \frac{1 + e^{\frac{d-v_{red}}{e}}}{1 + e^{\frac{b-v_{red}}{c}}}. \quad (2)$$

It can be seen that, in the limit of simultaneous fragment emission, the size of the Coulomb hole can be explained within the QMD+SMM approach if a volume parameter between  $\kappa = 2$  and  $10$  is used; both the results with  $\kappa = 1$  and  $\kappa = 15$  clearly disagree with the data for the heavier fragments. This means that these correlation functions are consistent with a simultaneous break-up with a Freeze-Out density of  $\rho = 0.1 - 0.3 \rho_0$ . For the lightest fragments the smallest volume parameter seems to describe the data best, but here the sensitivity to the Freeze-Out volume is less pronounced. This may indicate that the fragments do not come from a single Freeze-Out volume, but that the smaller fragments are emitted earlier from a smaller volume.

These results are in good agreement with previous investigations of the same data using the sequential three-body trajectory code MENEKA [16]. In this case an emission time of order  $500 \text{ fm/c}$  was found for a fixed freeze-out volume equivalent to  $\kappa = 1$ . These time scales are comparable to the typical time a fragment needs to traverse a Freeze-Out volume of roughly 5 times the nuclear volume.

Another feature that can be observed in the calculated correlation functions in figure 2 is the pronounced enhancement at a  $v_{red} \approx 15 - 20$ . This additional correlation is absent in the present light fragment data and is not seen in the data of the MSU group [18] except for very peripheral collisions [22]. Our calculations also show that this effect is more pronounced for larger impact parameters and increases (see figure 2) with decreasing SMM volume parameter (a similar behavior has recently been found in the Berlin model [23] when the excitation energy is decreased). A similar correlation was recently observed for the Au + Au reaction at 150

A MeV bombarding energy [24]. In this case the enhancement has its origin in the collective flow of the fragments. In our case, however we are dealing with a more asymmetric reaction at lower energies where the collective flow vanishes due to the compensation of the repulsive and attractive nuclear forces. However, the Coulomb repulsion due to a heavy third fragment can produce an additional correlation in the fragment–fragment correlation function. In table 1 we show the average charge of the largest fragment as well as the average charge asymmetry  $\langle \Delta Z \rangle = \sqrt{((Z_1 - Z_2)^2 + (Z_1 - Z_3)^2 + (Z_2 - Z_3)^2)/3}$  and the average multiplicity of IMF's with  $Z=4-20$  for values of  $\kappa$  from 1 to 15 over the impact parameter interval 0-6 fm in the reaction Fe (100 A MeV) + Au. It can be seen that the charge distribution gets very asymmetric with decreasing  $\kappa$  and the average IMF multiplicity decreases by a factor of two (the same holds also when the impact parameter is increased for a fixed volume parameter). This is a strong indication that the enhancement in the calculated correlation functions in figure 2 results from a large charge asymmetry.

The fact that the experimental data in ref. [16] does not show such an enhanced peak indicates that the break up pattern in nature is more symmetric than described within the SMM model. In order to clarify this point we show in figure 3 the experimental data for events with three detected IMF's. For this subset of the data, only the two lightest fragments are used to generate the correlation functions; the heaviest fragment is simply tagged as  $Z_{max}$ . The curves in Fig. 3 have been generated based on the following  $Z_{max}$  selection criteria: a) the numerator in eq. 1 contains only pairs from events with  $Z_{max} \geq 18$  (note however that this refers to the largest detected fragment) (dotted line), while no requirement has been applied to the fragments in the background pairs (the denominator in eq. 1); b) both the correlated and the background pairs are from events with detected  $Z_{max} \geq 18$  (dashed line); c) no cuts on  $Z_{max}$  (full line).

One clearly observes that, in accordance to the QMD+SMM results, a large peak is found for the trigger condition a) due to the recoil of a heavy third fragment which is not accounted for in the background. This peaks goes away when the background fragments are taken from events with a similar charge asymmetry. The full line shows again that the enhancement virtually disappears when no cuts are made on  $Z_{max}$ .

We have shown that the fragment–fragment reduced velocity correlation functions can be explained within the two–step model QMD+SMM, where the initial, dynamical step of the reaction, modeled using the microscopic QMD approach, is followed by a simultaneous statistical multifragmentation. The correlation functions for the system Fe (100 A MeV,  $b=0-6$ fm) + Au are consistent with a simultaneous break–up with a Freeze–Out density of  $\varrho = 0.1 - 0.3 \varrho_0$ . These findings are consistent with previous investigations assuming a sequential emission of the fragments from a fixed volume source. The typical time scale for this process was found to be less than 500 fm/c. We note that these time scales are comparable to the typical time a fragment needs to traverse a Freeze–Out volume of roughly 5 times the nuclear volume. The calculations show a additional correlation due to the coulomb repulsion from a heavy third fragment in an asymmetric decay. This effect is less pronounced in the experimental data, unless one explicitly triggers on pairs from events with a large charge asymmetry.

### Acknowledgements:

This work was supported by the US Department of Energy by LLNL under Contract W-7405-ENG-48. One of us (G.P.) gratefully acknowledges support from the Wissenschaftsausschuss of the NATO via the DAAD.

## References

- [1] J.E. Finn et al., A.S. Hirsch, A.T. Minich, B.C. Stringfellow, and F. Turkot, Phys. Rev. Lett. **49**, 1321 (1982); R.W. Minich et al., J.E. Finn, L.J. Gutay, A.S. Hirsch, and B.C. Stringfellow, Phys. Lett. B **118**, 458 (1982).
- [2] X. Campi, Phys. Lett. B **124**, 8 (1984); J. Phys. A **19**, L917 (1986) and Phys. Lett. B **208**, 351 (1988).
- [3] Y. Yariv and Z. Fraenkel, Phys. Rev. C **20**, 2227 (1979) and Phys. Rev. C **24**, 488 (1981); K.K. Gudima and V.D. Tonnev, Yad. Fiz. **27**, 67 (1978) [Sov. J. Nucl. Phys. **27**, 67 (1978)].
- [4] G. Peilert et al., W. Greiner, Phys. Rev. C **39**, 1402 (1989); Phys. Rev. C **37**, 2451 (1988).
- [5] G. Peilert et al., M.G. Mustafa Phys. Rev. C **46**, 1457 (1992).
- [6] J.J. Molitoris, H. Stöcker, and B.L. Winer, Phys. Rev. C **36**, 220 (1987); (1983); Y. Raffray, Nucl. Phys. A **465**, 317 (1987).
- [7] M. Blann, Phys. Rev. Lett. **54**, 2215 (1985) and Phys. Rev. C **32**, 1231 (1985); Phys. Rev. C **40**, 2498 (1989); G. Peilert, H. Stöcker, and W. Greiner, Phys. Rev. C **44**, 431 (1991).
- [8] R.J. Charity et al., Nucl. Phys. A **453**, 371 (1988); D.R. Bowman et al., ibid. A **523**, 386 (1991).
- [9] W.A. Friedman, Phys. Rev. Lett. **60**, 2125 (1988).
- [10] G. Fai and J. Randrup, Nucl. Phys. A **381**, 557 (1982) and Nucl. Phys. A **404**, 551 (1983).
- [11] J.P. Bondorf et al., H. Schulz, and K. Sneppen, Nucl. Phys. A **443**, 321 (1985); J.P. Bondorf et al., Nucl. Phys. A **444**, 460 (1985).
- [12] A.S. Botvina et al., R. Donangelo, and K. Sneppen, Nucl. Phys. A **475**, 663 (1987); A.S. Botvina, A.S. Iljinov, and I.N. Mishustin, Nucl. Phys. A **507**, 649 (1990).
- [13] D.H.E. Gross and X.Z. Zhang, Phys. Lett. B **161**, 47 (1985); D.H.E. Gross, X.Z. Zhang, and S.Y. Xu, Phys. Rev. Lett. **56**, 1544 (1986);
- [14] D. Hahn and H. Stöcker, Nucl. Phys. A **476**, 718 (1988).

- [15] B. Tsang et al., Phys. Rev. Lett. **71**, 1502 (1993).
- [16] T.C. Sangster et al., Th. Blaich, Prog. Part. Nucl. Phys. Vol. 30, 189 (1993) and Phys. Rev. C **47**, R2457 (1993) .
- [17] R. Lacey et al., Phys. Rev. Lett. **24**, 3705 (1993).
- [18] Y.D. Kim et al., Phys. Rev. C **45**, 338 (1992); C.K. Gelbke, W.G. Gong, and S. Pratt Phys. Rev. C **45**, 387 (1992).
- [19] S.E. Koonin, Phys. Lett. B**70**, 43 (1977); W.G. Gong et al., Phys. Rev. C**43**, 781 (1991).
- [20] A. Elmaani et al., Nucl. Instrum. Methods A**313**, 401 (1992).
- [21] T.C. Sangster et al., R.G. Lanier, S. Kaufman, W. Greiner, Phys. Rev. C**46**, 1404 (1992).
- [22] D.R. Bowman et al., C.K. Gelbke, W. G. Gong, Y.D. Kim, M.A. Lisa, M.B. Tsang, C. Williams, N. Colonna, K. Hanold, M.A. McMahan, G. Wozniak, and L.G. Moretto, Phys. Rev. Lett. **23**, 3534 (1993).
- [23] O. Schapiro, A.R. DeAngelis, and D. Gross, Preprint HMI 1993/P1-Schap 1.
- [24] B. Kämpfer et al., Phys. Rev. C**48** , R955 (1993).

## Figure Captions:

Figure 1:

Projections of the semi-exclusive triple differential cross section  $d^2\sigma/dZd\Omega$  for the reaction Fe (100 A MeV) + Au. The symbols show the data [21] for the fragment charge distributions at  $\vartheta_{Lab} = 72^\circ$  (upper panel) and the fragment angular distributions for  $Z = 10$  (lower panel). The histograms show the calculations with the QMD+SMM ( $b = 0 - 6$  fm) model for different volume parameters,  $\kappa$ , as indicated.

Figure 2:

Mixed fragment reduced velocity correlation functions for three different constraints on the Coulomb product  $Z_1 \cdot Z_2$ . The symbols show the data of ref. [16], while the curves are fits to equation 2 obtained with the QMD+SMM model. The different lines show calculations done with the volume parameter  $\kappa = 1$  (solid line),  $\kappa = 2$  (variable length dashed line),  $\kappa = 5$  (dashed line),  $\kappa = 10$  (dash-dotted line) and  $\kappa = 15$  (dotted line),

Figure 3:

Experimental correlation function for the lightest two fragments in events with three detected IMF's. The full line shows the fit to the correlation function obtained from all events while for the dotted line includes only events in which the largest of the three detected fragments has a charge greater than 17. The dashed line shows the fit when both the true and background pairs are from events with  $Z_{max} \geq 18$  (dashed line).



## Tables:

$\kappa$	$\langle Z_{max} \rangle$	$\langle \Delta Z \rangle$	$\langle MUL_{Z=4-20} \rangle$
1	26.5	12.3	2.2
2	22.7	10.5	2.7
5	18.8	8.2	3.4
10	17.9	7.5	3.6
15	16.0	6.2	4.0

Table 1:

The average charge of the largest fragment as well as the average charge asymmetry  $\langle \Delta Z \rangle = \sqrt{((Z_1 - Z_2)^2 + (Z_1 - Z_3)^2 + (Z_2 - Z_3)^2)/3}$  and the average multiplicity of IMF's with  $Z=4-20$  for the reaction Fe (100 A MeV,  $b=0-6$  fm) + Au and values of  $\kappa$  from 1 to 15.

This figure "fig1-1.png" is available in "png" format from:

<http://arxiv.org/ps/nucl-th/9312008v1>

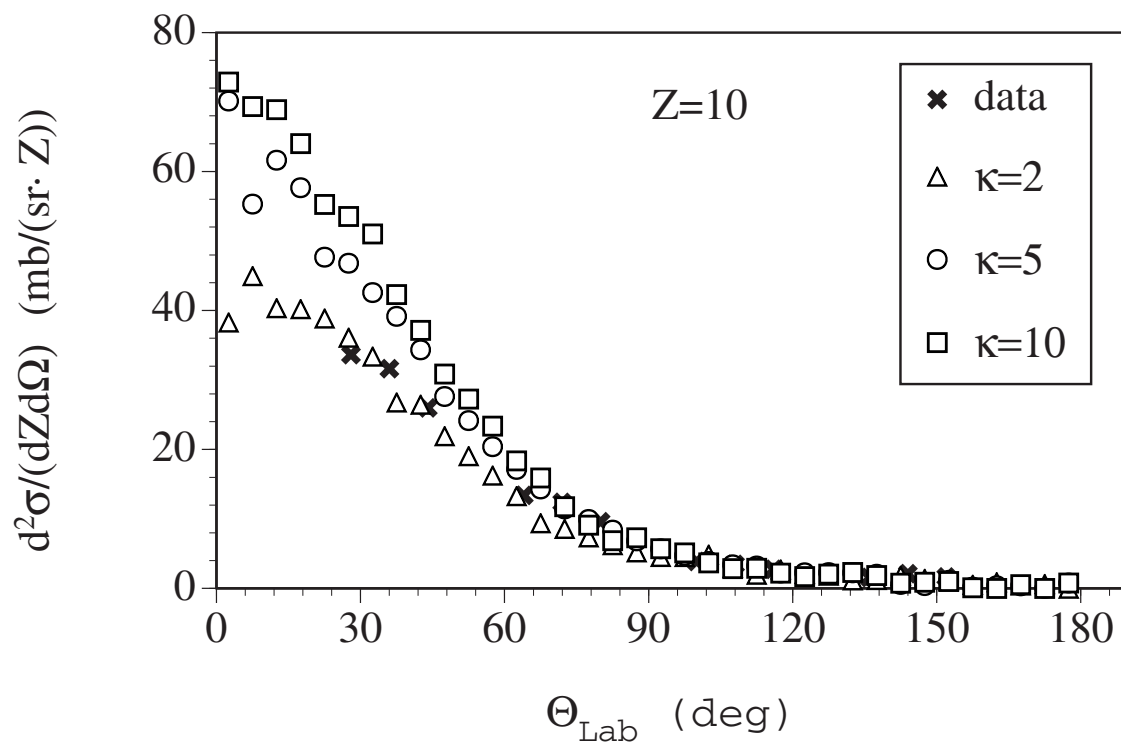
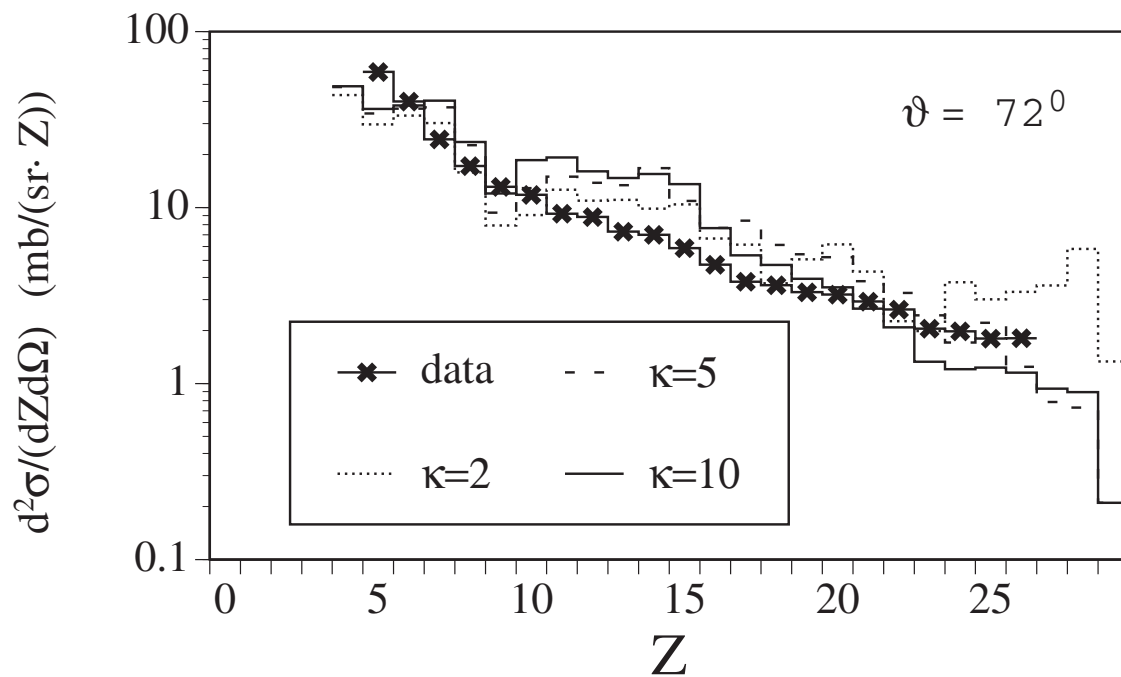
This figure "fig2-1.png" is available in "png" format from:

<http://arxiv.org/ps/nucl-th/9312008v1>

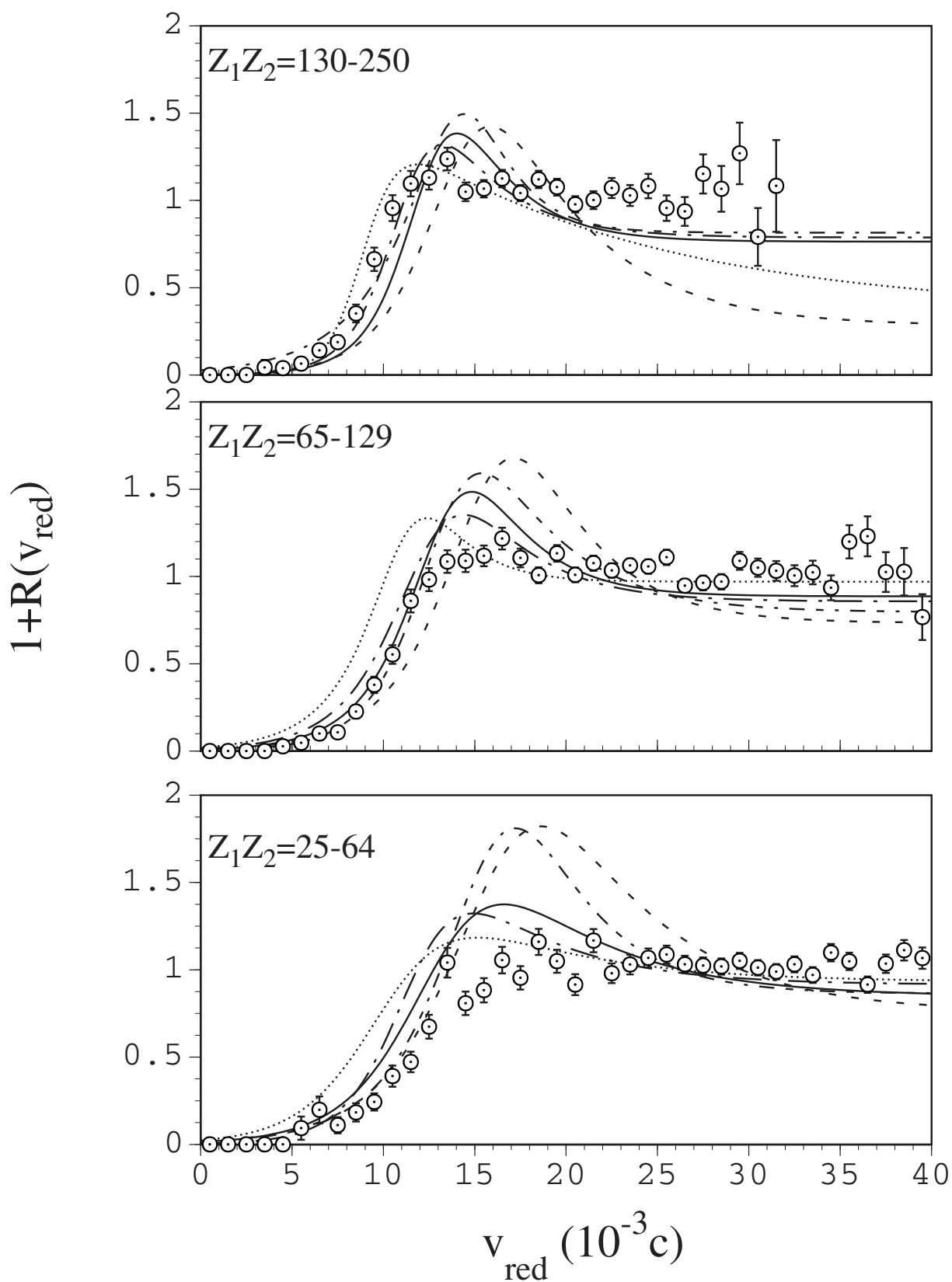
This figure "fig3-1.png" is available in "png" format from:

<http://arxiv.org/ps/nucl-th/9312008v1>

# Fe (100 A MeV) + Au



# Fe (100 A MeV) + Au



# Fe (100 A MeV) + Au

